

# UC Davis

## UC Davis Previously Published Works

### Title

A coadapted KNL1 and spindle assembly checkpoint axis orchestrates precise mitosis in Arabidopsis

### Permalink

<https://escholarship.org/uc/item/5ws5h4cq>

### Journal

Proceedings of the National Academy of Sciences of the United States of America, 121(2)

### ISSN

0027-8424

### Authors

Deng, Xingguang

He, Ying

Tang, Xiaoya

et al.

### Publication Date

2024-01-09

### DOI

10.1073/pnas.2316583121

Peer reviewed



# A coadapted KNL1 and spindle assembly checkpoint axis orchestrates precise mitosis in Arabidopsis

Xingguang Deng<sup>a,1,2</sup> , Ying He<sup>a,1</sup>, Xiaoya Tang<sup>a,1</sup>, Xianghong Liu<sup>a</sup>, Yuh-Ru Julie Lee<sup>b</sup> , Bo Liu<sup>b,2</sup> , and Honghui Lin<sup>a,2</sup>

Edited by Carolyn G. Rasmussen, University of California, Riverside, CA; received September 27, 2023; accepted November 30, 2023 by Editorial Board Member Natasha V. Raikhel

The kinetochore scaffold 1 (KNL1) protein recruits spindle assembly checkpoint (SAC) proteins to ensure accurate chromosome segregation during mitosis. Despite such a conserved function among eukaryotic organisms, its molecular architectures have rapidly evolved so that the functional mode of plant KNL1 is largely unknown. To understand how SAC signaling is regulated at kinetochores, we characterized the function of the *KNL1* gene in *Arabidopsis thaliana*. The KNL1 protein was detected at kinetochores throughout the mitotic cell cycle, and null *knl1* mutants were viable and fertile but exhibited severe vegetative and reproductive defects. The mutant cells showed serious impairments of chromosome congression and segregation, that resulted in the formation of micronuclei. In the absence of KNL1, core SAC proteins were no longer detected at the kinetochores, and the SAC was not activated by unattached or misaligned chromosomes. Arabidopsis KNL1 interacted with SAC essential proteins BUB3.3 and BMF3 through specific regions that were not found in known KNL1 proteins of other species, and recruited them independently to kinetochores. Furthermore, we demonstrated that upon ectopic expression, the KNL1 homolog from the dicot tomato was able to functionally substitute KNL1 in *A. thaliana*, while others from the monocot rice or moss associated with kinetochores but were not functional, as reflected by sequence variations of the kinetochore proteins in different plant lineages. Our results brought insights into understanding the rapid evolution and lineage-specific connection between KNL1 and the SAC signaling molecules.

KNL1 | SAC | kinetochore | Arabidopsis

Mitosis results in the production of two daughter cells with identical genomes by faithfully segregating sister chromatids at anaphase. Chromosomes are attached to spindle microtubules at kinetochores that are physically connected to centromeric nucleosomes. Errors in chromatid segregation resulted from incorrect attachment can lead to losses or gains of chromosomes in daughter cells that become aneuploid. Cells monitor chromosome biorientation until all kinetochores of sister chromatids are attached to microtubule fibers emanated from opposite spindle poles. Monitoring such amphitelic attachment is the spindle assembly checkpoint (SAC) which is activated by unattached chromosomes (1). SAC signaling is brought about by a suite of BUB (budding uninhibited by benzimidazoles), MAD (mitotic arrest deficient), or BMF (BUB1/MAD3 Family proteins in plants) proteins that catalyze the inhibition of the CDC20 protein which acts as the activator of the APC/C (Anaphase Promoting Complex/Cyclosome) (2, 3). Satisfaction of the SAC, as marked chromosome congression at the metaphase plate, is required for anaphase onset when CDC20 activates the APC/C to degrade cyclin B and other proteins (2, 4).

The SAC signaling proteins associate with kinetochores via direct binding to protein complexes that are assembled onto the centromere of each chromosome during mitosis (2). Namely, there are three evolutionarily conserved protein complexes known as kinetochore scaffold 1 (KNL1), minichromosome instability 12 (MIS12) complex, and nuclear division cycle 80 (Ndc80) complex, and they form the KMN network (5, 6). While the plant Ndc80 and MIS12 proteins are highly homologous to their animal counterparts, plant KNL1 homologs are related to their animal counterparts in two functional domains but share very little if any homology in the rest of the amino acid sequences (7, 8). For example, the plant KNL1 homologs lack the repetitive Met–Glu–Leu–Thr (MELT) motifs found in animal origins (9). The signature array of MELT repeats in the middle region of the animal KNL1, upon phosphorylation by the MPS1 (monopolar spindle 1), serves as the hubs for gathering BUB and MAD proteins at the kinetochores for SAC signaling (10). The homology between plant and animal KNL1 proteins lies in the coiled-coil domain followed by the C-terminal RWD domain (11). Unlike KNL1 proteins of the animal origin, the maize KNL1 interacts with BMF1 and BMF2 through a novel ~145-amino acid region outside the conserved domains but does not interact with either

## Significance

As a scaffold for kinetochore assembly, kinetochore scaffold 1 (KNL1) functions in recruiting spindle assembly checkpoint (SAC) components among many well-studied eukaryotes from yeasts to humans. Plants have acquired many unique features associated with SAC, how KNL1 assembles proteins at kinetochores and regulates mitosis in plants remains poorly understood. Our work addresses this knowledge gap through analyzing the *knl1* knockout mutants, determining its physical and genetic interactions with known and novel SAC proteins. We reveal that Arabidopsis KNL1 has evolved a specialized mechanism of functioning with SAC proteins to govern mitotic fidelity in a lineage-specific manner. The adaptability of KNL1 to generate specific checkpoint connections suggests an evolutionary strategy for creating diversity in plant reproduction and growth.

Author contributions: X.D., B.L., and H.L. designed research; X.D., Y.H., and X.T. performed research; X.D., X.L., and Y.-R.J.L. contributed new reagents/analytic tools; X.D., Y.H., X.T., X.L., Y.-R.J.L., B.L., and H.L. analyzed data; and X.D., B.L., and H.L. wrote the paper.

The authors declare no competing interest.

This article is a PNAS Direct Submission. C.G.R. is a guest editor invited by the Editorial Board.

Copyright © 2024 the Author(s). Published by PNAS. This article is distributed under [Creative Commons Attribution-NonCommercial-NoDerivatives License 4.0 \(CC BY-NC-ND\)](https://creativecommons.org/licenses/by-nc-nd/4.0/).

<sup>1</sup>X.D., Y.H., and X.T. contributed equally to this work.

<sup>2</sup>To whom correspondence may be addressed. Email: xgdeng@scu.edu.cn, bliu@ucdavis.edu, or hhlin@scu.edu.cn.

This article contains supporting information online at <https://www.pnas.org/lookup/suppl/doi:10.1073/pnas.2316583121/-/DCSupplemental>.

Published January 3, 2024.

BMF3 or BUB3 in a yeast two-hybrid assay (9). Therefore, the plant SAC proteins at kinetochores must be constructed into an interactive network different from that in animal or fungal cells.

In line with the sequence divergence of plant KNL1 homologs from their counterparts from other kingdoms, the BMF proteins also have limited homology to animal BUB1/MAD3 proteins, mostly in the N-terminal tetratricopeptide repeat (TPR) domain (12). The TPR domain is essential for the maize BMF1 and BMF2 proteins to interact with KNL1 (9). Intriguingly, the BMF1/2-binding domain found in the maize KNL1 is conserved in monocots only but similar regions exhibit high sequence divergence in eudicots (9). In contrast to animal and fungi, BMF1 and BMF2 do not interact with BUB3 in maize (9). There are two different classes of BUB3 proteins like BUB3.1/BUB3.2 and BUB3.3 in the model plant *Arabidopsis thaliana*. BUB3.1 and BUB3.2 are more closely related to BUB3 of fungal and animal origins than BUB3.3. BUB3.1/BUB3.2, however, interact with the microtubule-associated protein MAP65-3 and play critical roles in phragmoplast microtubule reorganization during cytokinesis but not in SAC signaling (13). In contrast, BUB3.3 probably is a SAC protein because of its oryzalin hypersensitive phenotype linked to the inactivation of the *BUB3.3* gene (12).

In *A. thaliana*, different SAC proteins exhibit different localization dynamics during mitosis. Among them, only BMF3 and MAD1 exhibit canonical, unattached kinetochore-dependent localization patterns while most others continuously appear at kinetochores and BMF2 is cytosolic (12). Furthermore, BMF1, unlike BMF2 and BMF3, does not play a critical role in SAC signaling although it is the only BMF protein possessing a kinase domain (12, 14). Thus, it has been enigmatic how these proteins may be associated with SAC signaling in the context of kinetochores and whether distinct assembly modes are accountable for SAC signaling in different land plants.

Studies carried out in both *Physcomitrium patens* and maize support the notion that the plant KNL1 plays a role in the faithful segregation of sister chromatids during mitosis (7, 9). However, the sequence divergence between plant and animal SAC and KNL1 proteins as well as the discrepancies associated with protein–protein interaction patterns raised several additional questions. First, do the plant KNL1 homologs serve the function in SAC signaling as their animal counterparts? If so, does it serve as a scaffolding factor for engaging BUB3.3 and BMF proteins at kinetochores for SAC signaling? Why do some SAC proteins exhibit different localization dynamics from others like their animal counterparts that dissociate from kinetochore when the SAC is turned off? Do different BMF proteins depend on different scaffolding factors at kinetochores? From an evolutionary perspective, do highly divergent KNL1 family proteins, as revealed by sequence comparisons, function differently in different plant lineages?

These questions prompted us to pursue the potentially divergent SAC regulatory mechanisms in plants. To do so, we performed a comprehensive functional analysis of the *KNL1* homolog in *A. thaliana* and uncovered a distinct functional scheme employed by KNL1 to promote SAC signaling through independently loading BMF3 and BUB3.3 on kinetochores, and such a critical function cannot be replaced by the KNL1 orthologs from bryophytes and even monocots.

## Results

**The *KNL1* Gene Is Important but Dispensable for Vegetative Growth and Reproduction.** A published study showed that the *zmknl1* mutation in maize caused mitotic defects in the developing

endosperm that consequently results in the production of small kernels (9). We wished to gain insights into the connection between the plant KNL1 protein with SAC signaling and plant growth by taking advantages of the sophisticated genetics and experimental agility of the model system *A. thaliana* in which the AT2G04235 locus was identified to encode a KNL1 homolog. Based on the SIGnAL record, the SALK\_068970 line was annotated to carry a T-DNA insertional mutation in the 8th intron which is designated as *knl1-1* here (Fig. 1*A*). We successfully recovered from the seed pool homozygous *knl1-1* offspring that was viable but had retarded growth. Because this T-DNA insertion was located toward the 3' region of the *KNL1* coding sequence, we generated other two additional alleles, *knl1-2<sup>cr</sup>* and *knl1-3<sup>cr</sup>*, using the CRISPR/Cas9 genome editing technology. The *knl1-2<sup>cr</sup>* and *knl1-3<sup>cr</sup>* mutations had 1 and 5-base pair deletions in the second exon, which led to the introduction of premature stop codons (Fig. 1*A*). All the three lines were *knl1* null mutants as the *KNL1* expression was undetectable in these mutants (*SI Appendix, Fig. S1*).

The three homozygous mutant plants exhibited identical macroscopic defects at various developmental stages. They were extremely dwarf and produced deformed dark/purple-colored rosette leaves that were barely expanded and incomparable to those of the wild-type (WT) plants (Fig. 1*B* and *C*). Although these mutants eventually were able to undergo sexual reproduction following limited vegetative growth, their fully expanded siliques had approximately a half of the space occupied by aborted seeds (44.2% for *knl1-1*,  $n = 512$ ; 46.0% for *knl1-2<sup>cr</sup>*,  $n = 534$ ; 47.1% for *knl1-3<sup>cr</sup>*,  $n = 508$ ) while the WT control had the space fully filled with healthy seeds (98.5%,  $n = 486$ ) (Fig. 1*D* and *E*). Specifically, most ovules from *knl1* mutants failed to develop normal embryos after fertilization (*SI Appendix, Fig. S2A*). To understand the underlying causes of reduced fertility, we analyzed male and female gametophyte development in *knl1* mutants. Pollen viability staining revealed increased inviable and shrunken grains compared to WT (*SI Appendix, Fig. S2B*). DAPI-stained pollen showed abnormal nuclear morphologies, and meiotic tetrads uncovered unbalanced microspore numbers (*SI Appendix, Fig. S2 D and E*). Female gametogenesis also exhibited irregular nuclear numbers and shapes in megagametophytes/embryo sacs (*SI Appendix, Fig. S2C*). These defects provided developmental explanations for the elevated seed abortion phenotype of *knl1* mutants. Furthermore, *knl1* mutants also formed leaf trichomes with increased branch numbers (Fig. 1*F*).

To confirm that the phenotypes described above were linked to the loss of *KNL1* function, genetic suppression/complementation experiments were performed in the *knl1-1* mutant background. Pleiotropic growth defects caused by the mutation were suppressed completely to the WT level by expressing a *KNL1*-GFP under the control of the native *KNL1* promoter (Fig. 1 and *SI Appendix, Fig. S3*), suggesting the phenotypes were indeed caused by the loss of *KNL1* and the fusion protein was functional.

**KNL1 Is a Constituent Kinetochore Protein Throughout the Mitotic Cell Division Cycle.** Because the *KNL1*-GFP fusion protein was functional, we examined subcellular localization of KNL1 during mitosis via immunofluorescence. For 180 detected cells from three independent rescue lines ( $n = 180$ ,  $N = 3$ ), *KNL1*-GFP signal was concentrated in discrete foci in interphase cells bearing transverse cortical microtubules (Fig. 2*A*), suggesting that kinetochore proteins were already assembled on centromeres as single dots associated with densely packed heterochromatin inside the nucleus before the cells entered mitosis, unlike M-phase-dependent assembly phenomenon found in mammalian

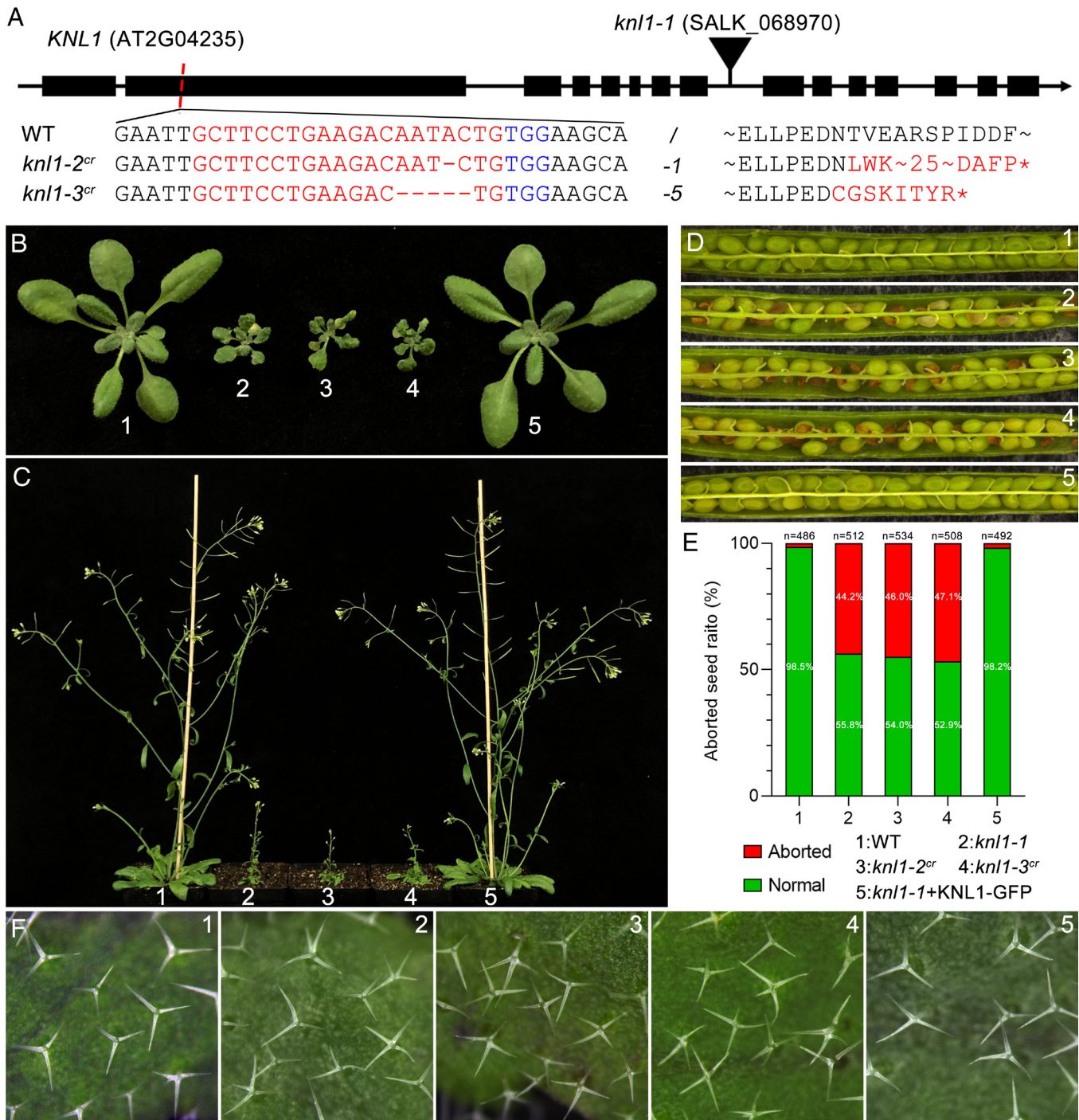


**Fig. 1.** KNL1 plays a critical role in vegetative growth and reproduction in *Arabidopsis*. (A) The diagram illustrates the gene structure of *KNL1* (At2g04235) with exons in boxes and introns in lines. The position of T-DNA insertion and gene editing site are indicated in the diagram. The sgRNA target sequence and changes in the *knl1-2<sup>cr</sup>* and *knl1-3<sup>cr</sup>* sequences are highlighted in red. Mutant transcripts are predicted to introduce premature stop codons (\*) resulted from frameshifts. (B) Comparison of the 3-wk-old plants of wild-type (WT) plant (1), *knl1-1* mutant (2), *knl1-2<sup>cr</sup>* mutant (3), *knl1-3<sup>cr</sup>* mutant (4), and *knl1-1* plant expressing the KNL1-GFP fusion protein (5). (C) Three *knl1* mutant alleles show serious growth reduction when compared to the WT and rescued plants grown for 6 wk. (D) The *knl1* mutants have frequently aborted seeds in the opened siliques. (E) Quantification of seed production in WT ( $n = 486$ ), *knl1* mutants ( $n = 512, 534, 508$ ), and rescued plants ( $n = 492$ ). (F) The *knl1* mutants frequently produce 4-pronged trichome while the WT and rescued plants have primarily 3-pronged trichomes on the leaf surface.

and yeast cells. The KNL1-GFP signal became paired dots in cells bearing the preprophase band (Fig. 2 B and C), suggesting that such a cell was at G2 phase or early prophase. Following nuclear envelope breakdown, paired KNL1-GFP dots were associated with heterochromatin surrounded by a bipolar spindle (Fig. 2D). At metaphase when chromosomes were aligned at the equatorial plate, the KNL1-GFP signal was detected at the two edges of aligned chromosomes where kinetochore fibers ended (Fig. 2E).

When kinetochore fibers shortened in anaphase, the KNL1-GFP dots separated into two groups and dislocated away from each other and eventually reached two spindle poles at telophase (Fig. 2 F and G). The prominent KNL1 signal remained as single bright foci in the two reformed daughter nuclei upon the completion of cell division (Fig. 2H). Therefore, we concluded that it KNL1 was associated with kinetochores throughout the cell division cycle in *Arabidopsis* cells.

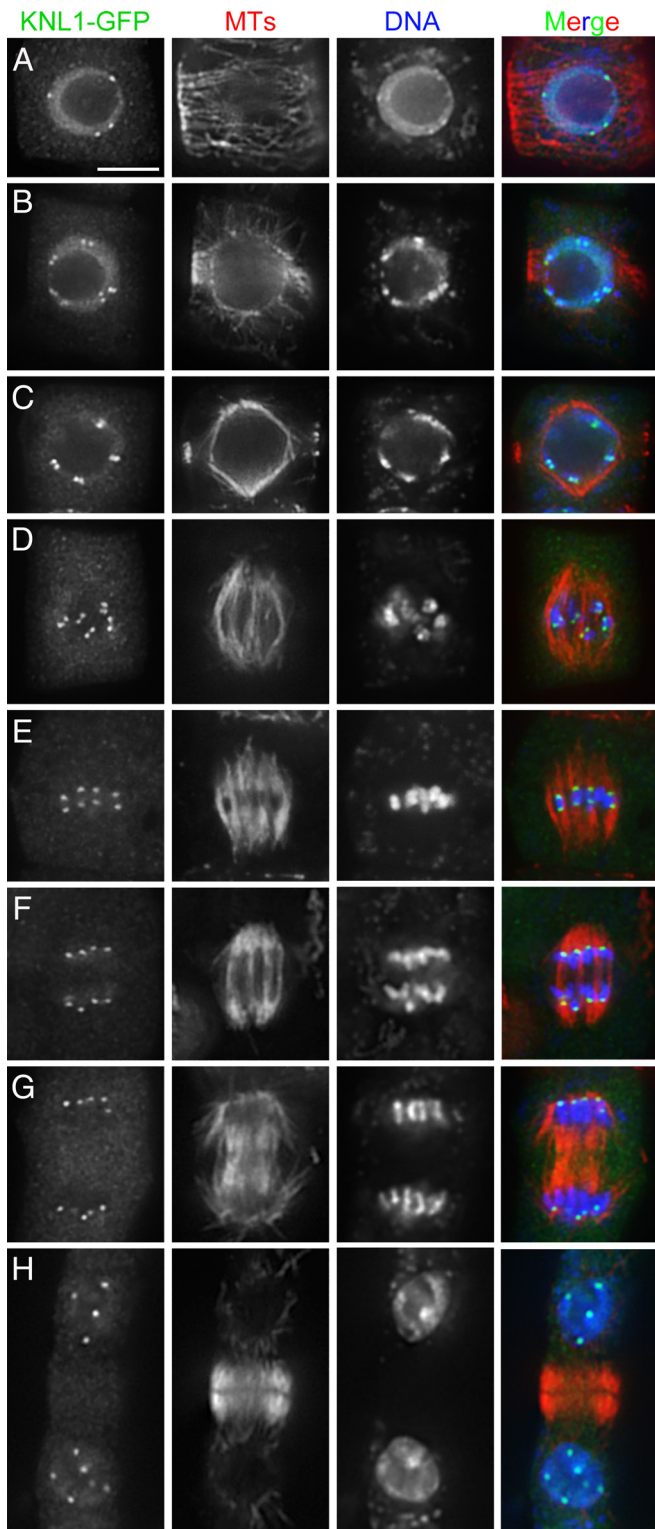


**Fig. 2.** Localization of KNL1-GFP during mitosis in *Arabidopsis*. (A) At interphase, KNL1 is concentrated at discrete foci in the nucleoplasm. (B) Paired KNL1 signal can be detected in cells bearing the preprophase band microtubule array. (C) At late prophase when a spindle microtubule array is detected, KNL1 appears exclusive in paired kinetochores. (D and E) The KNL1 pairs associate with chromosomes following nuclear envelope breakdown, and later exhibit biorientation at the metaphase plate and are connected to paired kinetochore fiber microtubules. (F) At anaphase, the KNL1 signal highlights kinetochores of the separated sister chromatids. (G and H) After arriving at spindle poles at telophase, KNL1 foci later become suspended in the nucleus when daughter nuclei are formed during cytokinesis. The merged images have KNL1-GFP detected by the anti-GFP antibody in green, microtubules in red, and DNA in blue. Micrographs are representative of 100% mitotic cells ( $n = 180$ ) from three independent transgenic lines ( $N = 3$ ). (Scale bars, 5  $\mu\text{m}$ .)

### KNL1 Plays a Critical Role in Faithful Chromosome Segregation.

The kinetochore localization of KNL1 prompted us to test whether its loss led to errors in mitosis. We examined microtubules and chromatin in mitotic cells of the *knl1-1* mutant and control plants by immunofluorescence. Compared to the WT cells that produced typical bipolar spindles with chromosomes perfectly aligned at the metaphase plate, the *knl1-1* mitotic cells that formed similar bipolar spindle arrays often had a few chromosomes positioned close to spindle poles while others had already been aligned at the metaphase plate (arrowheads, Fig. 3A). Quantitatively, the *knl1-1* mutant had 62.4% ( $n = 165$ ) of mitotic cells showing such chromosome misalignment phenotype which was never detected among WT control cells (0%,  $n = 150$ ) (Fig. 3C). We then asked how the mutant cells responded to the presence of uncongressed chromosomes by examining cytokinetic cells. While cytokinesis in 100% ( $n = 150$ ) of WT cells resulted in the birth of two daughter nuclei with identical size, 33.3% ( $n = 165$ ) of *knl1-1* cytokinetic cells produced micronuclei that were separated from the larger daughter nuclei and sometimes multiple micronuclei of different sizes were formed in each daughter cell (arrowheads, Fig. 3B and C). To analyze how the loss of KNL1 affected ploidy index globally, we measured DNA contents by flow cytometry. Compared to the WT control that had nuclei distributed in three major peaks of 2C, 4C, and 8C, the nuclei from the *knl1-1* mutant appeared in two conspicuous peaks at ploidy levels between 2C/4C and 4C/8C (*SI Appendix*, Fig. S4). The results suggested that *knl1-1* plants exhibit increased aneuploidy, likely due to defects in chromosome segregation during mitosis.

To further investigate abnormal chromosome segregation in the mutant cells by live-cell imaging, a Histone H1.2-RFP marker labeling chromosomes and a GFP-TUB6 marker labeling microtubules were delivered into the mutant and control plants so that chromosome/chromatid motility could be observed concomitantly with spindle remodeling. In WT cells, chromosomes congressed toward the middle of the developing spindle apparatus in an orchestrated manner and aligned at the metaphase plate that were flanked by paired kinetochore fibers after nuclear envelope breakdown. At anaphase, sister chromatids separated synchronously and grouped into two daughter nuclei separated by microtubule bundles in the spindle midzone and later the developing phragmoplast (100% of 16 cases) (Fig. 3D and *Movie S1*). In mitotic cells of *knl1-1* mutant, however, isolated chromosomes did not join the majority that congressed toward the metaphase plate in the middle of the spindle array, and instead moved toward and eventually positioned at the spindle poles. Subsequently, anaphase onset was detected without having the misaligned chromosomes congressed toward the other aligned ones (45% of 20 cases) (arrowheads, Fig. 3E and *Movie S2*). Moreover, the mutant cells also exhibited abnormalities in chromosome segregation that were highlighted by chromosome bridges (25% of 20 cases) and lagging chromosomes (15% of 20 cases) at late stages of mitosis (*SI Appendix*, Fig. S5A and B and *Movies S4* and *S5*). Failed segregation of “sticky” chromosome bridges led to failures in separating two chromatin masses so that the cells did not produce two separate daughter nuclei after mitosis (*SI Appendix*, Fig. S5 and *Movie S4*). Collectively, 80% ( $n = 20$ ) of *knl1-1* mitotic cells exhibited chromosome missegregation phenotype which were never observed in WT cells (0%,  $n = 16$ ) (*SI Appendix*, Fig. S5C).

To analyze chromosome motility in *knl1-1* cells, we followed individual chromosomes during anaphase and had their centroids tracked and plotted from their initial positions over time. A few lagging chromosomes displayed unsynchronized moves toward spindle poles while most sister chromatids segregated in an orchestrated manner (Fig. 3F). The lagging chromosomes moved

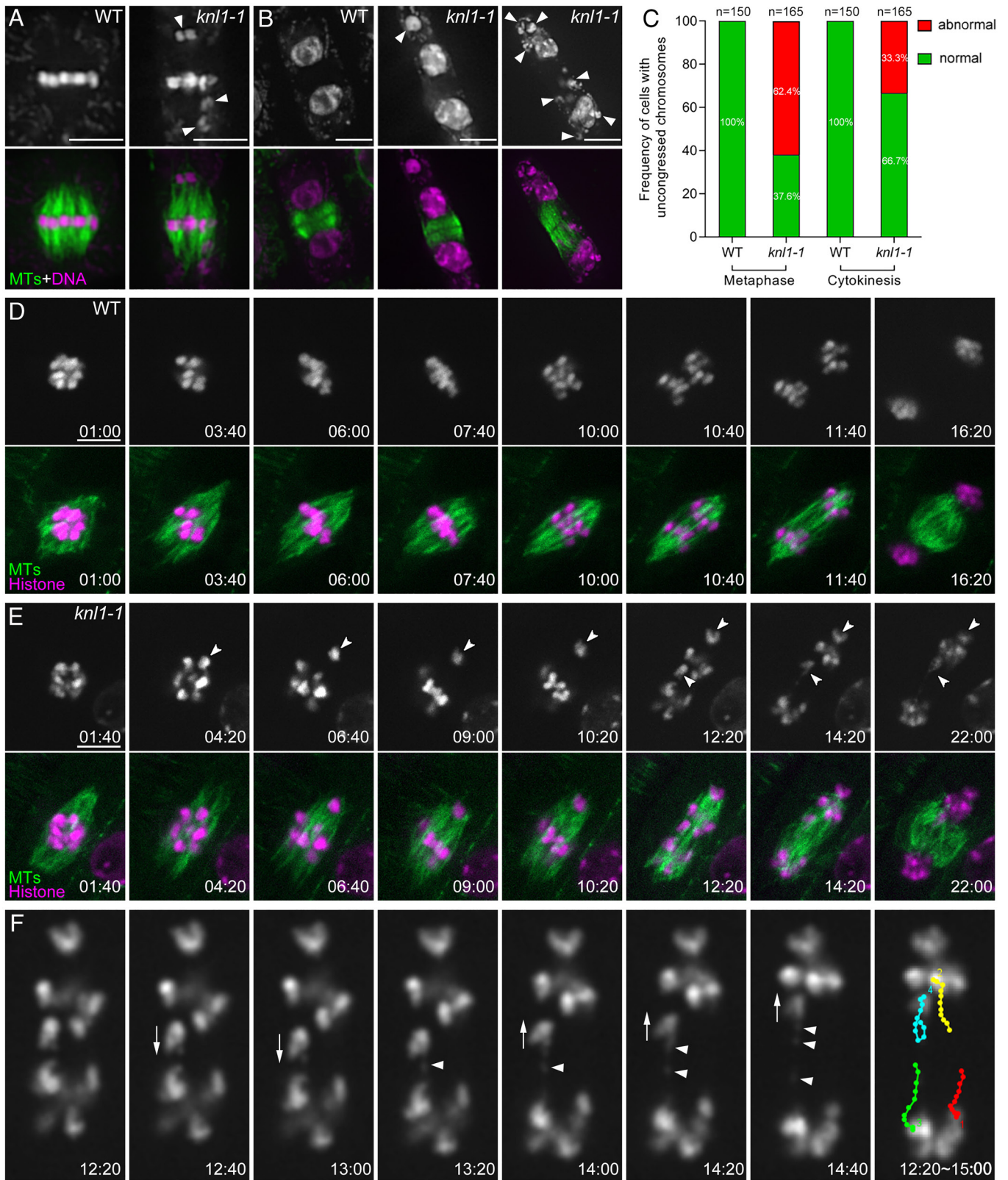


**Fig. 3.** KNL1 plays a critical role in chromosome congression and segregation. (A) Comparative views of chromosome alignment in WT and *knl1-1* mutant cells at metaphase. Misaligned chromosomes are indicated by white arrowheads in the *knl1-1* cells. (B) Comparative views of cytokinetic cells in WT and *knl1-1* plants. One or more micronuclei caused by KNL1 depletion are indicated by white arrowheads. Merged images have microtubules in green and DNA in magenta. (C) Quantitative assessment of cells exhibiting misaligned chromosomes at metaphase and cells producing micronuclei following cytokinesis in WT ( $n = 150$ ) and *knl1-1* plants ( $n = 165$ ). (D) Live-cell imaging of WT cells expressing GFP-TUB6 and Histone-RFP. Representative snapshot images are acquired from [Movie S1](#). (E) Live-cell imaging of *knl1-1* cells expressing GFP-TUB6 and Histone-RFP. Images are acquired from [Movie S2](#). Misaligned chromosomes and lagging chromosomes are indicated by arrowheads. (F) Representative time-lapse images of chromosome migration in *knl1-1* cells. Chromosome centroids are plotted distant from the initial position over time, and the movement of individual chromosomes is tracked by lines using different colors in the *Last* panel. Arrows show the direction of chromosome migration; arrowheads point at chromosome bridges. Live-cell images are representative of 16 mitotic videos from WT ( $n = 16$ ) and 20 mitotic videos from *knl1-1* ( $n = 20$ ) plants. (Scale bars, 5  $\mu\text{m}$ .)

backward to the metaphase plate or associated with the chromatid mass that was destined to the opposite pole. While most sister chromatids were segregated synchronously toward opposite poles, the lagger later corrected its movement toward the pole in proximity of its initial position (Fig. 3F and Movie S3). We interpreted that such a chromosomal instability phenomenon in *knl1-1* cells might be stem from errors in kinetochore amphitelic attachment.

**KNL1 Is Essential for the Recruitment of Critical SAC Proteins to Kinetochores.** Because the *knl1* mutant had mitosis proceeded with unaligned chromosomes, we hypothesized that SAC signaling was deficient in the absence of KNL1. To test this hypothesis, we first challenged the plants with oryzalin as a characteristic phenotype of the loss of an essential SAC component led to hypersensitivity to microtubule-depolymerizing drugs (12). We found that oryzalin at 100 nM significantly exacerbated the short root phenotype associated with the *knl1-1* seedlings, as quantitatively reflected by the measurement of root lengths ( $1.41 \pm 0.12$  cm for mock versus  $0.56 \pm 0.03$  cm for treatment,  $n = 18$ ), while the identical condition did not noticeably alter the growth

of the WT seedlings ( $3.04 \pm 0.18$  cm for mock versus  $2.95 \pm 0.05$  cm for treatment,  $n = 18$ ) (Fig. 4 A and B). The oryzalin-inhibited growth phenotype in the *knl1-1* mutant was completely repressed again by the expression of the KNL1-GFP fusion protein (Fig. 4 A and B), indicating that the phenotype was linked to the inactivation of *KNL1* in the mutant.

The KNL1 protein provides the key platform for recruiting MAD and BUB proteins to kinetochores in animals and fungi (15). Such discrepancy prompted us to test whether the Arabidopsis KNL1 protein shared the platform role as its fungal and animal counterparts. To do so, we focused on the localization of BUB and MAD proteins, which have been reported to be kinetochore-localized when fused with GFP (12, 16), including GFP-BUB3.3, BMF1-GFP, BMF3-GFP, and GFP-MAD1. The kinetochore localization of GFP-BUB3.3 (Fig. 4 C and D), BMF3-GFP (Fig. 4 G and H) and GFP-MAD1 (Fig. 4 I and J) detected in the control cells were completely abolished in the *knl1-1* mutant cells ( $n \geq 100$ ,  $N = 3$ ), indicating that the KNL1 protein was required for the recruitment of these SAC important proteins to kinetochores in Arabidopsis. In contrast, we found that BMF1 localized to kinetochores throughout mitosis was not

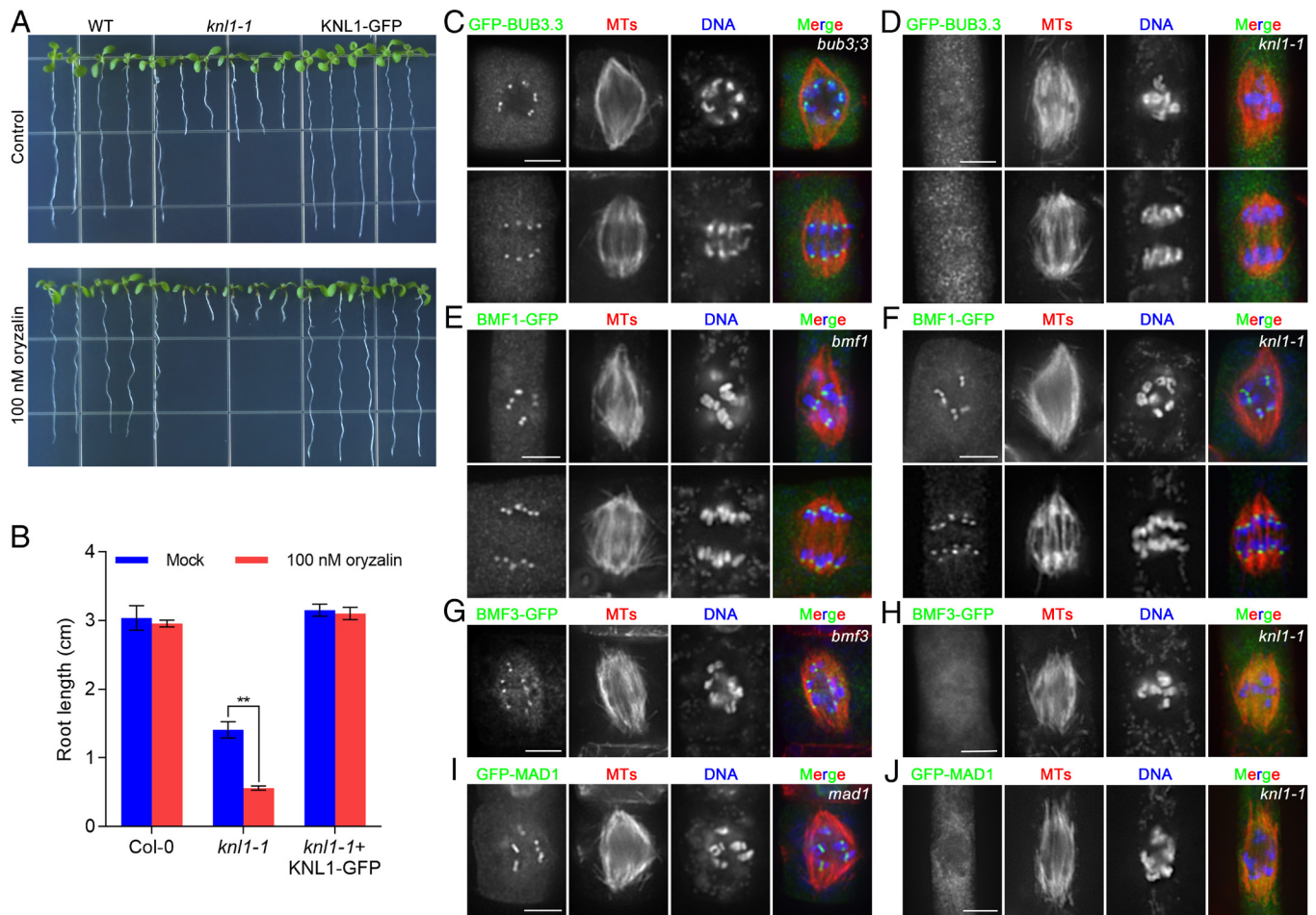


**Fig. 4.** KNL1 is essential for kinetochore localization of core SAC proteins in *A. thaliana*. (A) Comparison of seedlings of the WT, *knl1-1* mutant, and *knl1-1* mutant expressing KNL1-GFP with and without 100 nM oryzalin treatment after grown for 10 d. (B) Quantification of root lengths in the seedlings in (A) with and without oryzalin treatment. Data are means  $\pm$  SD measured from three independent experiments ( $N = 3$ ) each containing six individual measurements ( $n = 6$ ). \*\* indicates significance ( $P < 0.01$ , pairwise comparison using one-way ANOVA analysis). (C and D) GFP-BUB3.3 localized to kinetochores upon expression in the *bub3.3* mutant (C) but becomes diffuse in the cytoplasm in the *knl1-1* mutant cells (D) at prometaphase (Top) and anaphase (Bottom). (E and F) BMF1-GFP is detected at kinetochores upon expression in the *bmf1* mutant (E) and in *knl1-1* mutant cells (F) in representative cells at prophase (Top row) and anaphase (Bottom row). (G and H) BMF3-GFP localization is shown at kinetochore when expressed in the *bmf3* mutant (G) and becomes diffuse in the *knl1-1* mutant cells (H). (I and J) GFP-MAD1 localizes to kinetochores upon expression in the *mad1* mutant (I) and becomes diffuse in the cytoplasm in the *knl1-1* mutant cells (J). Merged images have GFP-tagged proteins in green, microtubules in red, and DNA in blue. Micrographs are representative of more than 100 cells from three independent lines ( $n \geq 100$ ,  $N = 3$ ) with similar results. (Bars, 5  $\mu$ m.)

affected in *knl1-1* mutant cells ( $n \geq 100$ ,  $N = 3$ ) and similar to what was observed in the control cells (Fig. 4 E and F). Because BMF1 probably is not a critical SAC component in plants, our results suggested that KNL1 probably was required for the kinetochore localization of critical SAC components.

**KNL1 Selectively Interacts with BUB3.3 and BMF3.** Because the SAC critical components depended on KNL1 for their kinetochore localization, we then asked whether the dependence was brought about by interactions between KNL1 and SAC proteins. Yeast two-hybrid (Y2H) and bimolecular fluorescence complementation (BIFC) assays revealed KNL1 interacted with BUB3.3 and BMF3, but not BMF1, BMF2, MAD1, and MAD2 (Fig. 5 A and B). To identify the determinant(s) of BUB3.3 and BMF3 binding in KNL1, we generated constructs for a set of truncated variants of KNL1 protein (Fig. 5 C). First, we separated KNL1 into two parts, the half N-terminal region (KNL1<sup>1-724</sup>) and the remaining C-terminal fragment (KNL1<sup>725-1227</sup>) and found that the KNL1<sup>1-724</sup> fragment was sufficient for the interaction with both BUB3.3 and BMF3 (Fig. 5 D). The interaction domain was further narrowed down to the region including residues 1–295 and its immediate flanking sequences did not contribute to the interaction (Fig. 5 D). We then performed extensive Y2H experiments using truncation fragments of KNL1<sup>1-295</sup> and found that deletion of residues 131–295 in KNL1<sup>1-295</sup> abolished these interactions (Fig. 5 D). Because the KNL1 family proteins in land plants showed poor overall sequence conservation, even between eudicots and monocots. The amino acid sequence of Arabidopsis KNL1 was aligned with orthologs from eudicots including tomato, cotton, and soybean. We found the regions corresponding to amino acids 105–262 in Arabidopsis KNL1

exhibited higher conservation than the rest of these KNL1 homologs of different eudicots (SI Appendix, Fig. S6), hence they were named eudicot-specific-domain (ESD). When this ESD was removed, KNL1 failed to interact with either BUB3.3 or BMF3 in Y2H, BIFC, and in vitro pull-down experiments (Fig. 5 D–F). These results indicate that the ESD was required for KNL1 to bind BUB3.3 and BMF3.

We then examined the functionality of the ESD in vivo by expressing the truncated KNL1<sup>ΔESD</sup> under its native promoter in the *knl1-1* homozygous background. In contrast to the full length of KNL1, the truncate lacking the ESD failed to suppress the growth defects in the *knl1-1* mutant (Fig. 6 A and SI Appendix, Fig. S3). In contrast to the mutant cell expressing full-length KNL1 which progressed through mitosis with accurate chromosome segregation, *knl1* cells with the truncated KNL1<sup>ΔESD</sup> protein showed unaligned chromosomes that were associated with missegregation at anaphase (arrowheads, Fig. 6 B). We then asked whether the ESD region was required for KNL1 localization to kinetochores and found that the truncated KNL1<sup>ΔESD</sup>-FLAG fusion protein localized similarly as full-length KNL1-FLAG (Fig. 6 C and D). To further test whether this region was essential for recruiting BUB3.3 and BMF3 to kinetochores, we had BUB3.3 and BMF3 GFP fusions coexpressed with either KNL1 or KNL1<sup>ΔESD</sup> fused with FLAG in *knl1-1* background. While the full-length KNL1-FLAG rescued kinetochore loading of both BUB3.3-GFP and BMF3-GFP in *knl1-1* cells ( $n \geq 100$ ,  $N = 3$ ), KNL1<sup>ΔESD</sup>-FLAG, although detected at kinetochores, did not restore the kinetochore staining of either BUB3.3 or BMF3 ( $n \geq 100$ ,  $N = 3$ ) (Fig. 6 C and D). This result suggested that the ESD-mediated interaction with BUB3.3 and BMF3 was essential for these proteins to achieve kinetochore localization.

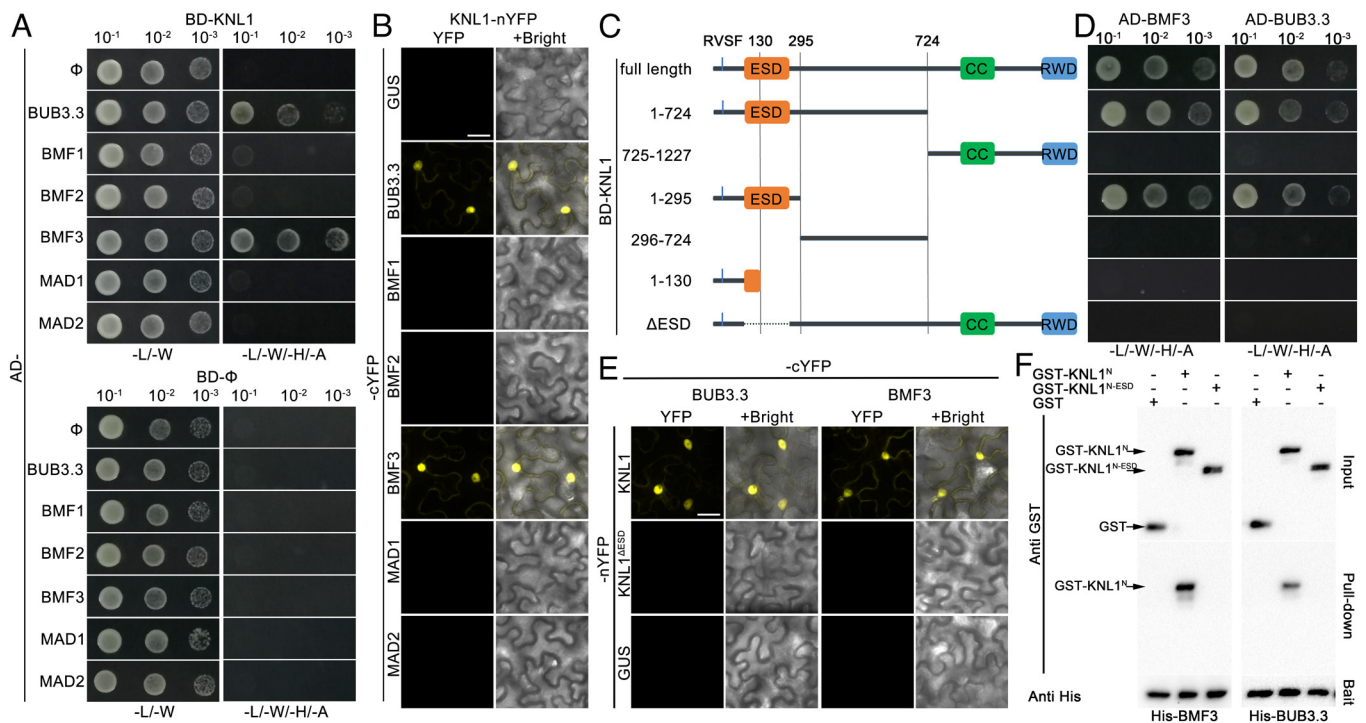


**Fig. 5.** KNL1 interacts with BUB3.3 and BMF3. (A) Assessment of interactions between KNL1 and SAC components by Y2H assays. The empty vector is used as a negative control ( $\emptyset$ ). The yeast cultures were spotted on vector-selective (-L/-W, *Left* column) and interaction-selective (-L/-W/-H/-A, *Right* column) media and photographed after incubation at 30 °C for 2 d. (B) Bimolecular fluorescence complementation (BIFC) assay examining interactions of KNL1 (fused with the N-terminal fragment of YFP) and SAC proteins (fused with the C-terminal fragment of YFP) in *Nicotiana benthamiana*. (C) Schematic representation of full-length and truncated versions of KNL1 used to map BUB3.3 and BMF3 binding domains. (D) Y2H interactions between truncated KNL1 variants and BMF3/BUB3.3. (E) BIFC assay to examine interactions between BUB3.3/BMF3 and truncated KNL1 variants. (F) In vitro pull-down assays of recombinant GST fusions of KNL1 variants with His-BMF3/BUB3.3 immobilized beads. BIFC experiments were repeated three times ( $N = 3$ ) with similar results. (Scale bars, 25  $\mu$ m.)



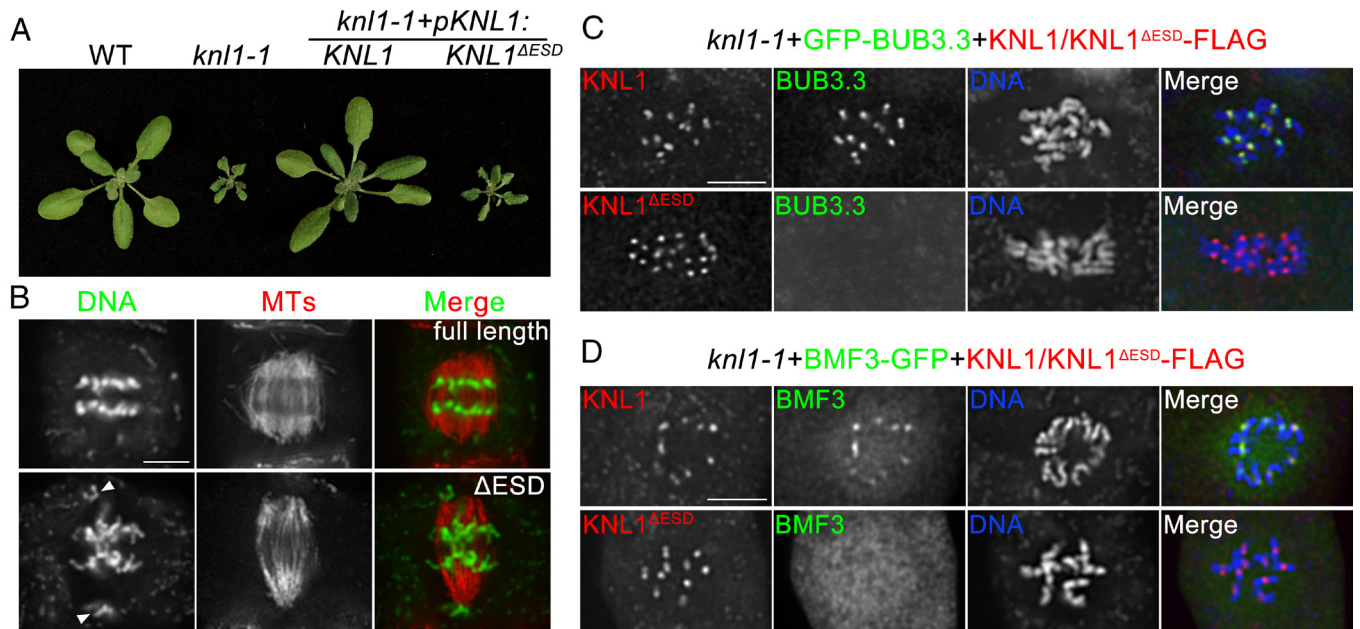


**Fig. 6.** KNL1 deploys a eudicot-specific domain to recruit BUB3.3 and BMF3 to kinetochores. (A) Growth phenotypes of 3-week-old plants of WT, *knl1-1*, and mutant plants expressing KNL1 and KNL1<sup>ΔESD</sup>. (B) Representative images of chromosome segregation in *knl1-1* mutant cells expressing KNL1-FLAG (Top rows) and KNL1<sup>ΔESD</sup>-FLAG (Bottom rows), misaligned chromosomes are indicated by white arrowheads. Merged images have microtubules in red and DNA in green. (C and D) Localization of GFP-BUB3.3 (C) and BMF3-GFP (D) in *knl1-1* mutant expressing KNL1-FLAG or KNL1<sup>ΔESD</sup>-FLAG. While both KNL1-FLAG and KNL1<sup>ΔESD</sup>-FLAG are detected at kinetochores, GFP-BUB3.3 and BMF3-GFP colocalize with KNL1-FLAG but not KNL1<sup>ΔESD</sup>-FLAG. The merged images have FLAG-tagging proteins detected by the FLAG antibody in red, GFP-tagging proteins detected by the GFP antibody in green, and DNA stained by DAPI in blue. Micrographs are representative of more than 100 cells from three independent transgenic lines with similar results ( $n \geq 100$ ,  $N = 3$ ). (Scale bars, 5  $\mu\text{m}$ .)

### Plant KNL1 Orthologs Display Lineage-Specific Connection with the SAC Signaling Molecules.

Because the BUB3.3- and BMF3-binding region of Arabidopsis KNL1 is conserved among eudicots but not in monocots, we then asked whether KNL1 family members in different plant lineages were functionally interchangeable. We chose *Oryza sativa* and *Solanum lycopersicum* as the representative of monocots and eudicots. The moss *P. patens* was also chosen for functional comparison of KNL1 family from this bryophyte representing early land plants. We delivered these three KNL1 orthologs into *knl1-1* mutant under the control of Arabidopsis *KNL1* promoter and found only *SlKNL1*, but not *OsKNL1* or *PpKNL1*, suppressed the dwarf-phenotype of *knl1-1* (Fig. 7A). We then examined intracellular localization of these KNL1 orthologs in the host cells of *A. thaliana*. Surprisingly, all these three KNL1 orthologs, even though the *OsKNL1* and *PpKNL1* were not functional, exhibited kinetochore association in Arabidopsis (Fig. 7B and C). Consistent with the functionality assay, only the *SlKNL1* protein was able to recruit BUB3.3 and BMF3 to kinetochores ( $n \geq 100$ ,  $N = 3$ ) (Fig. 7B and C). We further tested whether the possession or loss of the functionality of these KNL1 orthologs in *A. thaliana* cells was associated with the interaction with Arabidopsis BUB3.3 and BMF proteins. Y2H and BIFC assays reported that none of these proteins interacted with *AtBMF1* and *AtBMF2*. *SlKNL1* interacted with both *AtBUB3.3* and *AtBMF3* but not other *AtBMF* proteins, like the Arabidopsis KNL1. Interestingly, *OsKNL1* interacted with *AtBMF3*, but not *AtBUB3.3* (SI Appendix, Fig. S7). In contrast, the moss KNL1 did not interact with any of BUB/BMF proteins from Arabidopsis. These results collectively suggested that the sequence divergence among the plant KNL1 family proteins significantly changed the protein conformation and interaction properties so that the pairing of KNL1 with SAC signaling molecules acquired lineage-specific features associated with rapidly evolved interaction domains.

### Discussion

In this study, we demonstrated that the Arabidopsis KNL1 protein has acquired distinct functional features that were associated with its dicot-specific sequence architecture while preserving the fundamental function as a kinetochore scaffolding protein for recruiting critical SAC signaling molecules. The viable and fertile *knl1* null mutants in *A. thaliana* generated here offered us great advantages to uncover how this rapidly evolved protein acquired lineage-specific activities and how the protein was coupled with the regulation of SAC during mitosis. Our results also showed how the dynamics of different BUB3 and BMF family proteins were organized and orchestrated in the context of kinetochore localization and SAC signaling. Hence, the study brought insights into plant-specific features of SAC signaling, divergent from what has been appreciated in animal and fungal cells (15).

**Domain Architecture of the Plant KNL1 Proteins.** Despite being evolutionarily conserved as the SAC scaffolding factor at kinetochores, KNL1 family proteins display poor sequence conservation and variable protein sizes among previously examined eukaryotes (11, 17). These proteins may be divided into two sections, the N-terminal section serving as the loading dock for various SAC and perhaps other mitotic signaling molecules and the C-terminal part responsible for protein's kinetochore localization. Toward the N terminus, a variety of functional motifs including SILK, RVSE, and MELT and KI can be recognized among most if not all fungal and animal KNL1 homologs despite the high degree of sequence divergence (15, 17). Given the importance of these motifs for SAC signaling, only the RVSE motif is conserved among plant KNL1 homologs (11). Instead, many features were replaced by the rapidly evolving ESD domain in this region in *A. thaliana*. The lack of interaction between *OsKNL1* and BUB3 as well as BMF3 may reflect another variation regarding the interaction

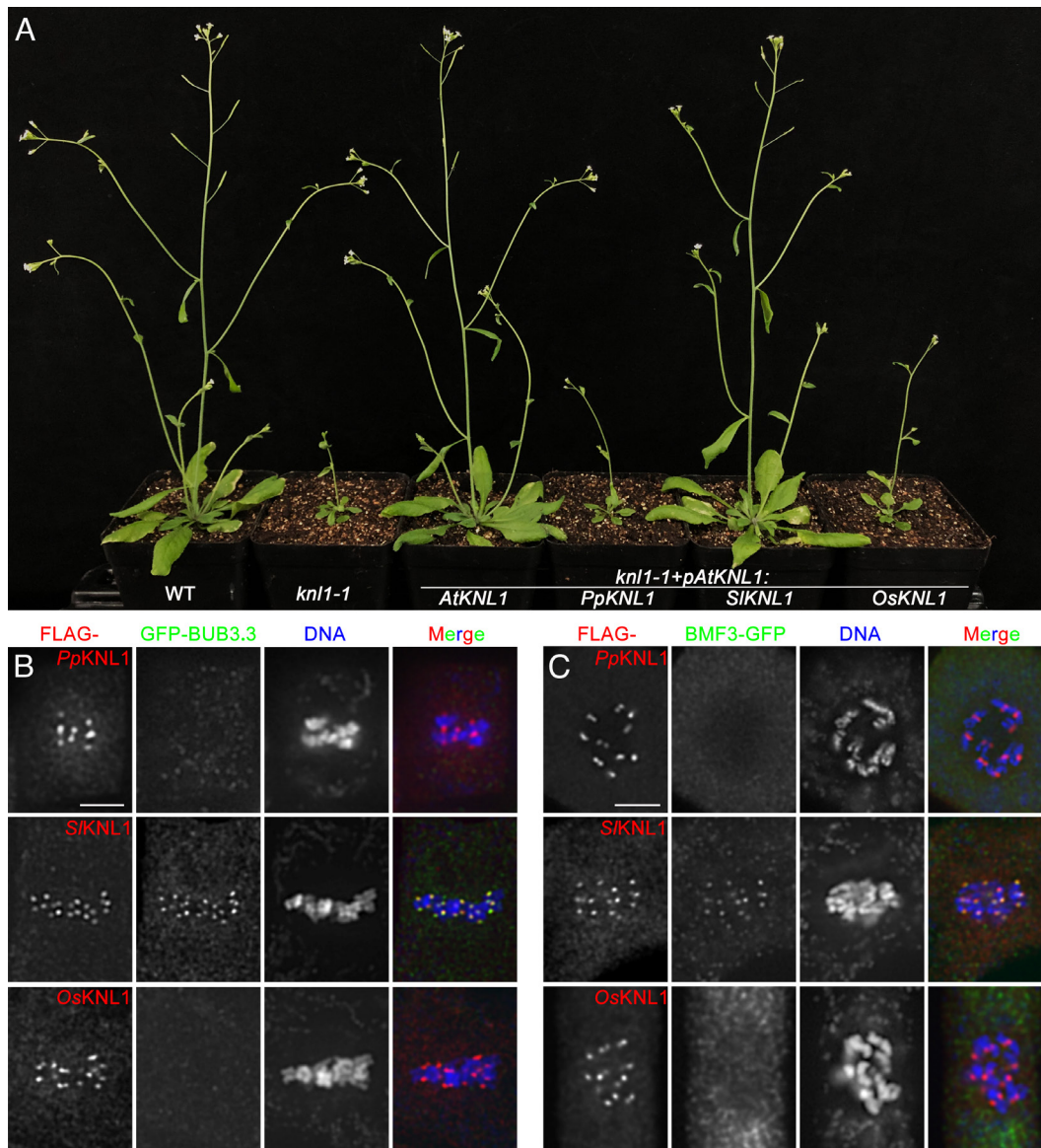


**Fig. 7.** KNL1 of a eudicot but not monocot or bryophyte origin captures the function in *A. thaliana*. (A) Growth phenotypes of 5-week-old plants of WT, *knl1-1*, and mutant plants expressing KNL1 orthologs from *P. patens*, *S. lycopersicum*, and *O. sativa*. *AtKNL1* is used as the positive control. (B and C) Assessment of the kinetochore localization of GFP-BUB3.3 (B) and BMF3-GFP (C) in *knl1-1* mutant cells expressing FLAG-tagged *PpKNL1*, *SIKNL1*, or *OsKNL1* detected by the anti-FLAG antibody. The merged images have FLAG-tagging proteins in red, GFP-tagging proteins in green, and DAPI-stained DNA in blue. Micrographs are representative of more than 100 cells from three independent transgenic lines ( $n \geq 100$ ,  $N = 3$ ) with similar results. (Scale bars, 5  $\mu\text{m}$ .)

between the KNL1 protein and SAC proteins in monocot species and nonflowering plants (9). Therefore, studies of KNL1 evolution in green photosynthetic organisms could be a fascinating subject. Given the difference in the KNL1-BMF interaction patterns, it would be equally interesting to learn how KNL1 is dynamically connected to different SAC signaling molecules among these organisms.

In contrast to the N-terminal part, the C-terminal half of the KNL1 proteins are more conserved by presenting a coiled-coil domain and the RWD domain, which are responsible for the identification of homologs in different organisms (11, 15). The coiled-coil domain of the animal KNL1 is known for the direct interaction with the Zwint protein in order to recruit the RZZ complex for the localization of cytoplasmic dynein. Coincidentally, flowering plants lack Zwint, RZZ complex proteins, and cytoplasmic dynein (18). Therefore, it is intriguing whether such an interaction module has been replaced by a novel one for KNL1

function at kinetochores in plants. In animal cells, kinetochore localization of KNL1 is determined by the RWD domain through direct interaction with NSL1 which is a component of the Mis12 complex (19, 20). However, there is no obvious NSL1 homolog in *A. thaliana* and other plants, which raised the question of whether the conserved RWD domain linked KNL1 to the Mis12 complex in Arabidopsis cells. Therefore, it is yet to be determined how a possible connection between KNL1 and Mis12 complex was established and what domain(s) in Arabidopsis KNL1 determined its kinetochore localization.

**Regulation of SAC Signaling by KNL1 in *A. thaliana*.** Earlier studies showed that SAC signaling molecules exhibit three different dynamic localization patterns, activated SAC-dependent kinetochore association, constituent kinetochore decoration, and cytosolic distribution (12, 21, 22). Unlike animal and fungal KNL1 proteins that localize to kinetochores most noticeably from

prophase to early telophase (15), the Arabidopsis KNL1 protein decorates kinetochores at interphase and throughout the mitotic cell cycle. It is intriguing how BMF3 which also interacted with KNL1 and relied on the later for its kinetochore localization acquired activated SAC-dependent localization. One potential mechanism is a phosphorylation-dependent mechanism, analogous to the MPS1-dependent MELT phosphorylation-dependent recruitment of BUB3 in animal cells (23). Two lines of evidence argue against such a possibility. First, MPS1 is not required for BMF3 localization although it likely still plays a role in SAC signaling as demonstrated by the oryzalin hypersensitivity phenotype linked to its loss (12). Second, BMF1, being the only one among the MAD and BMF proteins that bears a kinase domain, is dispensable in SAC signaling so that a BMF1-dependent phosphorylation event is not critical for BMF3 localization either (12, 14). Alternatively, such a mechanism could have been established through the centromere-localized Aurora kinase AUR3 which forms the chromosomal passenger complex like that shown in animal cells (24, 25). The lack of viable *aur3* mutants challenges a direct assay as done for other SAC signaling molecules through molecular genetics.

Here, we also showed that the kinetochore localization of MAD1 was dependent on KNL1 in *A. thaliana*. MAD1 requires BMF3 for its kinetochore localization (12). Therefore, MAD1 failed to localize to kinetochores in the *knl1* mutant cells perhaps because BMF3 was no longer recruited there. This again demonstrates a drastic difference from vertebrates in which MAD1 has multiple kinetochore receptors (26, 27). Unlike BMF3, BMF1 and BMF2 perhaps functioned independently to KNL1. This conclusion was based on three lines of evidence. First, KNL1 did not interact with BMF1 and BMF2. Second, BMF1 did not require KNL1 for its kinetochore localization. Lastly, BMF2 is a cytosolic protein and does not even assume kinetochore localization. Furthermore, the independence of BMF1's kinetochore localization to KNL1 also is echoed by its dispensability in SAC signaling. Collectively, our results suggested that the kinetochore localization of BUB3.3 and BMF3 via KNL1 was required for their functions in SAC signaling. Delocalization of BUB3.3 and BMF3 from kinetochores led to insufficient SAC signaling for preventing mitotic cells from entering anaphase in the presence of unaligned chromosomes.

Our findings in *A. thaliana* revealed differences from those of *ZmKNL1* reported in *Zea mays*. *ZmKNL1* interacts with BMF1 and BMF2 but not BMF3 from maize through an annotated coiled-coil domain (9). Surprisingly, the rice *OsKNL1* interacted with Arabidopsis BMF3 but not BUB3.3 even though the BUB3 family proteins are highly conserved in their primary amino acid sequences. This was perhaps consistent with the finding that *ZmKNL1* did not interact with maize BUB3. Our results also indicated that KNL1's function in SAC signaling required its role in recruiting both BUB3.3 and BMF3 as demonstrated by the tomato KNL1 homolog but not the rice counterpart. It would be interesting to investigate whether the monocot BMF1 and BMF2 homologs behave like their counterparts from *A. thaliana*, in terms of their localization and SAC functionality as well as their connection with KNL1 in vivo. Nevertheless, it would not be surprising that monocots and dicots perhaps wire SAC molecules differently at kinetochores because it has been demonstrated that different eukaryotic organisms other than plants deploy variable linker pathways to construct similar outer kinetochore structure (28). The differences in monocots and dicots may represent such diversity and plasticity of kinetochore structures.

**Phenotypic Difference between *knl1* and *bub3.3/bmf* Mutants.** Because anaphase onset was not delayed in the presence of misaligned chromosomes in the *knl1* mutant cells, kinetochore localization of

the SAC molecules or their kinetochore-dependent posttranslational modification like phosphorylation was critical for SAC activation. If KNL1 were solely devoted to SAC signaling, we would have expected that its mutants behaved similarly as the *bub3.3* or *bmf* mutants which did not exhibit noticeable growth difference from the WT plants prior to being challenged by oryzalin. However, the *knl1* mutants exhibited great degrees of growth retardation and compromised reproduction. This finding suggested that KNL1 functioned beyond recruiting BUB3.3 and BMF3 to kinetochores for SAC signaling. In fact, it is known that the N terminus of KNL1 family proteins is responsible for recruitment of the phosphatase PP1 to kinetochores for silencing SAC signaling prior to anaphase onset (29, 30). The RVSF motif which is known for PP1 interaction is conserved in plant KNL1 proteins, suggesting that such a PP1-related function might be conserved in plants as well. To our knowledge, it is unclear how PP1 homologs function in SAC signaling in flowering plants. In animal cells, compromised PP1-dependent SAC silencing leads to delayed metaphase (30). PP1 at kinetochores is also known to promote kinetochore-microtubule attachment (29, 31, 32). It does so by antagonizing Aurora B autophosphorylation at kinetochores so that the spindle and kinetochore-associated (Ska) complex can join the force with the Ndc80 complex for strengthening end-on microtubule binding (33, 34). Homologs of the three Ska subunits can be identified in plant genomes. In the moss *P. patens*, Ska1 is detected at metaphase kinetochores and its downregulation by RNAi induces misaligned and later lagging chromosomes during mitosis (7). Taken together, it was tempting to hypothesize that the serious defects in chromosome congression and unsynchronized sister chromatid segregation shown here in the *knl1* mutant might be due to compromised activities of the Ska complex at kinetochores. Unfortunately, putative Ska subunits have not been studied in *A. thaliana*. Future investigation of the complex and its potential connection with KNL1 could bring insights into mechanisms underlying kinetochore-microtubule attachment in flowering plants.

On the other hand, kinetochores were still assembled in the absence of KNL1 in *A. thaliana*, as highlighted by the BMF1-concentrated signal that were attached to kinetochore fibers. This result suggest that there are alternative, KNL1-independent mechanism(s) that govern kinetochore assembly in plants. Although KNL1 is often treated as the core scaffold for the assembly of outer kinetochore during the M phase in animal cells, other constitutively localized kinetochore/centromere protein known as CENPs may contribute to the process as well. For example, the vertebrate CENP-K protein functions redundantly in producing the kinetochores that are competent for docking the Ndc80 complex to kinetochores (35). Redundant kinetochore assembly pathways may explain the survival of *knl1* mutants in *A. thaliana*. In vertebrates, linking the KMN complexes to centromeres are proteins like CENP-C and CENP-TWSX as demonstrated (28). While a few CENP homologs like CENP-C, CENP-O, CENP-S, and CENP-X are found in *A. thaliana*, many other animal CENPs did not seem to have obvious plant homologs (7). In fact, homologs of CCAN and KMN proteins in different eukaryotic lineages likely exhibit great plasticity and limited conservation. Therefore, much of the plant kinetochore proteome are yet to be revealed and novel plant CENPs could be identified through perhaps copurifying binding partners of the KNL1 protein.

## Materials and Methods

**Plant Materials and Plasmid Construction.** T-DNA insertion mutant of *knl1-1* (SALK\_068970) was obtained from NASC, mutants of *knl1-2<sup>cr</sup>* and *knl1-3<sup>cr</sup>* were generated through the CRISPR/Cas9 system. Binary vectors were generated

via Gateway cloning for localization and complementation analyses. Details are provided in [SI Appendix, Materials and Methods](#).

**Protein Interaction Assays.** Candidate interactors were tested by Y2H, BIFC, and in vitro pull-down experiments. Details are provided in [SI Appendix, Materials and Methods](#).

**Phenotype Characterization.** Male and female gametophytes were examined by Alexander staining, ovule clearing, and tetrad observation. Details are provided in [SI Appendix, Materials and Methods](#).

**Microscopy.** Immunofluorescence, live-cell imaging, and fluorescence microscopy visualized protein localization and mitotic defects. Details are provided in [SI Appendix, Materials and Methods](#).

**Image Analysis.** Microscopic phenotypes were quantified from random cell samples ( $\geq 100$ ) across at least three biological replicates. Statistical comparisons used ANOVA. Details are provided in [SI Appendix, Materials and Methods](#).

**Data, Materials, and Software Availability.** All study data are included in the article and/or [supporting information](#).

**ACKNOWLEDGMENTS.** We thank Dr. Arp Schnittger and Dr. Shinichiro Komaki for the collaboration on spindle assembly checkpoint (SAC) and specifically for sharing the SAC plasmid, Dr. Peishan Yi for the *Physcomitrella patens* cDNA library, and Dr. Tsuyoshi Nakagawa for the pGWB vectors. This study was supported by NSF of China (32270354 and 31900163 to X.D.), NSF of Sichuan Province (2022NSFSC1651 to X.D.), Institutional Research Fund of Sichuan University (2020SCUNL212 to X.D. and H.L.), Sichuan Forage Innovation Team Program (scxtd-2020-16 to H.L.), and NSF of USA (1920358 to Y.-R.J.L. and B.L.)

Author affiliations: <sup>a</sup>Ministry of Education Key Laboratory for Bio-Resource and Eco-Environment, College of Life Sciences, State Key Laboratory of Hydraulics and Mountain River Engineering, Sichuan University, Chengdu 610064, China; and <sup>b</sup>Department of Plant Biology, College of Biological Sciences, University of California, Davis, CA 95616

1. N. London, S. Biggins, Signalling dynamics in the spindle checkpoint response. *Nat. Rev. Mol. Cell Biol.* **15**, 736–747 (2014).
2. P. Lara-Gonzalez, J. Pines, A. Desai, Spindle assembly checkpoint activation and silencing at kinetochores. *Semin. Cell Dev. Biol.* **117**, 86–98 (2021).
3. B. Liu, Y.-R.J. Lee, Spindle assembly and mitosis in plants. *Ann. Rev. Plant Biol.* **73**, 227–254 (2022).
4. A. Musacchio, The molecular biology of spindle assembly checkpoint signaling dynamics. *Curr. Biol.* **25**, R1002–R1018 (2015).
5. C. Sacristan, G. J. P. L. Kops, Joined at the hip: Kinetochores, microtubules, and spindle assembly checkpoint signaling. *Trends Cell Biol.* **25**, 21–28 (2015).
6. I. M. Cheeseman, J. S. Chappie, E. M. Wilson-Kubalek, A. Desai, The conserved KMN network constitutes the core microtubule-binding site of the kinetochore. *Cell* **127**, 983–997 (2006).
7. E. Kozgunova, M. Nishina, G. Goshima, Kinetochore protein depletion underlies cytokinesis failure and somatic polyploidization in the moss *Physcomitrella patens*. *eLife* **8**, e43652 (2019).
8. J. J. E. van Hooff, E. Tromer, L. M. van Wijk, B. Snel, G. J. Kops, Evolutionary dynamics of the kinetochore network in eukaryotes as revealed by comparative genomics. *EMBO Rep.* **18**, 1559–1571 (2017).
9. H. Su *et al.*, Knl1 participates in spindle assembly checkpoint signaling in maize. *Proc. Natl. Acad. Sci. U.S.A.* **118**, e2022357118 (2021).
10. M. Vleugel *et al.*, Sequential multisite phospho-regulation of KNL1-BUB3 interfaces at mitotic kinetochores. *Mol. Cell* **57**, 824–835 (2015).
11. E. Tromer, B. Snel, G. J. P. L. Kops, Widespread recurrent patterns of rapid repeat evolution in the kinetochore scaffold KNL1. *Genome Biol. Evol.* **7**, 2383–2393 (2015).
12. S. Komaki, A. Schnittger, The spindle assembly checkpoint in Arabidopsis is rapidly shut off during severe stress. *Dev. Cell* **43**, 172–185 (2017).
13. H. Zhang *et al.*, Role of the BUB3 protein in phragmoplast microtubule reorganization during cytokinesis. *Nat. Plants* **4**, 485–494 (2018).
14. M. Wang *et al.*, BRK1, a Bub1-related kinase, is essential for generating proper tension between homologous kinetochores at metaphase I of rice meiosis. *Plant Cell* **24**, 4961–4973 (2012).
15. G. V. Caldas, J. G. DeLuca, KNL1: Bringing order to the kinetochore. *Chromosoma* **123**, 169–181 (2014).
16. X. Deng *et al.*, The Arabidopsis BUB1/MAD3 family protein BMF3 requires BUB3.3 to recruit CDC20 to kinetochores in spindle assembly checkpoint signaling. *bioRxiv* [Preprint] (2023). <https://doi.org/10.1101/2023.06.22.545541> (Accessed 24 July 2023).
17. P. Ghongane, M. Kapanidou, A. Asghar, S. Elowe, V. M. Bolanos-Garcia, The dynamic protein Knl1–A kinetochore rendezvous. *J. Cell Sci.* **127**, 3415–3423 (2014).
18. V. Silió, A. D. McAinsh, J. B. Millar, KNL1-bubs and RZZ provide two separable pathways for checkpoint activation at human kinetochores. *Dev. Cell* **35**, 600–613 (2015).
19. A. Petrovic *et al.*, Modular assembly of RWD domains on the Mis12 complex underlies outer kinetochore organization. *Mol. Cell* **53**, 591–605 (2014).
20. A. Petrovic *et al.*, The MIS12 complex is a protein interaction hub for outer kinetochore assembly. *J. Cell Biol.* **190**, 835–852 (2010).
21. G. J. P. L. Kops, B. Snel, E. C. Tromer, Evolutionary dynamics of the spindle assembly checkpoint in eukaryotes. *Curr. Biol.* **30**, R589–R602 (2020).
22. S. Komaki, A. Schnittger, The spindle checkpoint in plants—A green variation over a conserved theme? *Curr. Opin. Plant Biol.* **34**, 84–91 (2016).
23. Y. Yamagishi, C.-H. Yang, Y. Tanno, Y. Watanabe, MPS1/Mph1 phosphorylates the kinetochore protein KNL1/SpC7 to recruit SAC components. *Nat. Cell Biol.* **14**, 746–752 (2012).
24. S. Komaki *et al.*, Functional analysis of the plant chromosomal passenger complex. *Plant Physiol.* **183**, 1586–1599 (2020).
25. S. Komaki *et al.*, Molecular convergence by differential domain acquisition is a hallmark of chromosomal passenger complex evolution. *Proc. Natl. Acad. Sci. U.S.A.* **119**, e2200108119 (2022).
26. Y. Luo, E. Ahmad, S.-T. Liu, MAD1: Kinetochore receptors and catalytic mechanisms. *Front. Cell Dev. Biol.* **6**, 51 (2018).
27. I. Leontiou *et al.*, The Bub1-TPR domain interacts directly with Mad3 to generate robust spindle checkpoint arrest. *Curr. Biol.* **29**, 2407–2414.e7 (2019).
28. S. Sridhar, T. Fukagawa, Kinetochore architecture employs diverse linker strategies across evolution. *Front. Cell Dev. Biol.* **10**, 862637 (2022).
29. B. Roy, V. Verma, J. Sim, A. Fontan, A. P. Joglekar, Delineating the contribution of Spc105-bound PP1 to spindle checkpoint silencing and kinetochore microtubule attachment regulation. *J. Cell Biol.* **218**, 3926–3942 (2019).
30. J. S. Rosenberg, F. R. Cross, H. Funabiki, KNL1/SpC105 recruits PP1 to silence the spindle assembly checkpoint. *Curr. Biol.* **21**, 942–947 (2011).
31. M. R. Audett *et al.*, The microtubule- and PP1-binding activities of *Drosophila melanogaster* Spc105 control the kinetics of SAC satisfaction. *Mol. Biol. Cell* **33**, ar1 (2022).
32. J. Espeut, D. K. Cheerambathur, L. Krenning, K. Oegema, A. Desai, Microtubule binding by KNL-1 contributes to spindle checkpoint silencing at the kinetochore. *J. Cell Biol.* **196**, 469–482 (2012).
33. D. Liu *et al.*, Regulated targeting of protein phosphatase 1 to the outer kinetochore by KNL1 opposes Aurora B kinase. *J. Cell Biol.* **188**, 809–820 (2010).
34. L. A. Helgeson *et al.*, Human Ska complex and Ndc80 complex interact to form a load-bearing assembly that strengthens kinetochore-microtubule attachments. *Proc. Natl. Acad. Sci. U.S.A.* **115**, 2740–2745 (2018).
35. I. M. Cheeseman, T. Hori, T. Fukagawa, A. Desai, KNL1 and the CENP-H/I/K complex coordinately direct kinetochore assembly in vertebrates. *Mol. Biol. Cell* **19**, 587–594 (2008).